Greek crosses, cut from the same wafer ($d = 0.56$ mm, $n = 3 \times 10^{17}$ cm^{-3}), as shown in Fig. 1.1.18 (Seabaugh and Bell, 1988). One set of these

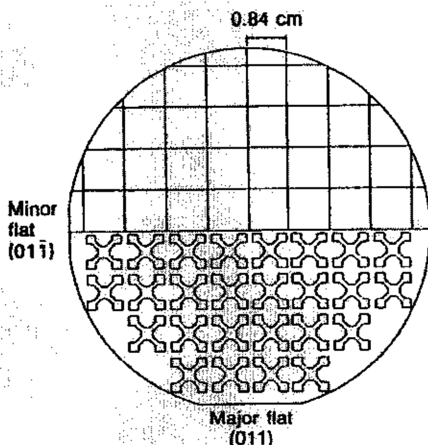

Fig. 1.1.18 A 3-inch, Si-doped, LEC GaAs wafer cut into square and cross patterns, as shown, for a round-robin investigation. (After Seabaugh and Bell (1988). Reproduced by permission of the National Bureau of Standards)

configurations was sent to each participating laboratory, with instructions to put on contacts according to the usual procedure used by that laboratory. As might be expected, some of the contacts were small and well defined, while others covered a rather significant portion of the sample. Each set of samples, with contacts, was then measured by the laboratory that put them on, and then was sent to several other laboratories. The results showed some systematic differences between the two structures, but fortunately they were small and not significant for most purposes. Thus, for GaAs samples in this thickness (~0.1 μm) and concentration range, it appears that the square shape can be used with confidence. However, results may be different for other thicknesses and concentrations. A full report on the round-robin study will be published later (Seabaugh and Bell, 1988).

1.1.7 Contacts

What should be the simplest part of a Hall-effect measurement, namely, putting on the contacts, is often the most troublesome. One would think that after more than 25 years of electrical measurements in GaAs, there would be a standard recipe or recipes which would produce good ohmic

contacts on any kind of GaAs. Unfortunately that is not the case, for several reasons: (1) requirements are changing, as contact dimensions are necessarily reduced for smaller devices, and as different materials and device structures are introduced; (2) the recipes cannot be made complete because unknown factors, e.g., polish damage, are variable and/or poorly understood; and (3) what is 'ohmic' for one application may not be ohmic for another application; in fact, even a reduction in temperature can sometimes change an ohmic contact into a non-ohmic contact. For GaAs Hall-effect measurements, the necessary currents range from about 10^{-12} to 10^{-1} A. But the resistance of a Hall device remains constant as the lateral dimensions are scaled down equally, and thus the current requirements should be the same. This means that the contact-current *density* in a small device is correspondingly larger than that in a large device, and thus the contact itself must have a lower 'specific contact resistivity' in order to be acceptable. Because of such problems, it is worthwhile to discuss ohmic contacts in some detail.

1.1.7.1 Definition of ohmic contact

There are many definitions of an ohmic contact, including the following:

(A) a perfect source and sink of both carrier types and having no tendency to inject or collect either electrons or holes;
(B) a source of carriers with an internal resistance R_c which is totally negligible compared with the semiconductor resistance;
(C) a source of carriers with a non-negligible internal resistance R_c, but one which obeys Ohm's law for current densities of interest.

Definition (A) has only academic significance since no actual contacts ever fulfill this condition. For purposes of this book, we will basically adopt either (B) or (C) as our definition. That is, if the total circuit resistance R_T is given as $R_T = 2R_c + r_s l/w$, where r_s is the sheet resistance, l the length, and w the width of the semiconductor material between the two contacts, then the contacts will be considered ohmic if R_T is independent of current magnitude and polarity. This condition could be satisfied in either of two ways: (1) $R_c \ll r_s l/w$, which is equivalent to definition (B); or (2) R_c itself is independent of current magnitude and polarity, which is definition (C). One ambiguity with our definition is that if R_T turns out to be non-ohmic, then we really don't know whether the problem is with R_c or r_s. That is, suppose an n-type semiconductor had an n–p–n junction somewhere between two ohmic contacts. Then r_s would probably not be ohmic, so that R_T would not be ohmic either, even though the contacts were. However, for Hall-effect measurements, we are not interested in the contacts themselves, only in ensuring that they not interfere with the measurements of V_c and V_H. In a few cases, definition (C) is not sufficient to give an *acceptable* contact even if

R_c is ohmic. That is, if R_c is so high that sufficient current cannot be passed to get good measurements of V_c and V_H, then the contact is not acceptable.

1.1.7.2 Theory of ohmic contacts

To quantify an ohmic contact, it is usual to employ one of the following 'figures of merit':

(1) the *specific contact resistance* $\rho_c(\Omega\text{-cm}^2)$, also known as the *specific contact resistivity*, the *contact resistivity*, or the *contact resistance*, in various sources; and
(2) the *normalized contact resistance*, or *specific transfer resistance*, which we will designate by $r_c(\Omega\text{-mm})$.

The first of these (ρ_c) has both theoretical and practical significance, while the second (r_c) has only a practical significance.

To illustrate the concept of specific contact resistance, consider the structure shown in Fig. 1.1.19(a), which consists of a semiconductor slab of

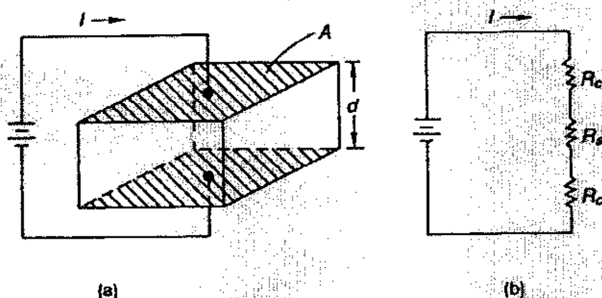

Fig. 1.1.19 (a) A simple structure and (b) equivalent circuit, for contact-resistance measurements

thickness d and area A, covered on top and bottom by the contacting metal. The simple equivalent circuit is shown in Fig. 1.1.19(b). It is clear that both the contact and bulk resistances will scale inversely with A, but only the bulk resistance will scale with a thickness (d, in this case), since the effective contact thickness is not even known. Thus, it seems natural to define $R_c = \text{constant}/A$, and the constant is called ρ_c, normally written in units of $\Omega\text{-cm}^2$. A formal definition of ρ_c is usually given as

$$\rho_c = \left\{ \frac{\partial j}{\partial V} \bigg|_{V=0} \right\} \Omega\text{-cm}^2 \qquad (1.1.27)$$

which will be discussed in more detail below.

The other figure of merit has application to planar contacts on a thin layer, as illustrated in Fig. 1.1.20. Here each contact has a definite area,

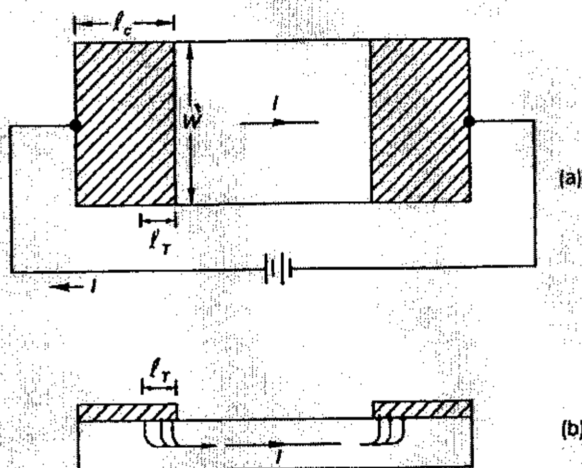

Fig. 1.1.20 An illustration of 'current crowding' in planar contacts. Here l_T is the *transfer length*: (a) planar view; (b) cross-sectional view

wl_c, but this area is not relevant under most circumstances. The reason is that the current does not flow uniformly out of the *whole* length of the contact l_c, but only from a length l_T, known as the *transfer length*. It is well known, and will be shown later, that $l_T = \sqrt{(\rho_c/R_s)}$, where R_s is the sheet resistance of the material under the contact, and thus the contact resistance is roughly given by $R_c = \rho_c/wl_T = \sqrt{(\rho_c/R_s)}/w$, as long as $l_T \leq 0.5l_c$. Usually, $l_T \ll l_c$, so that R_c is independent of l_c. Under these circumstances the area wl_c does not have much significance, but w itself still does, of course. Thus, a meaningful figure of merit would be given by $R_c =$ constant$/w \equiv r_c/w$, where the most common unit for r_c is Ω-mm. It must be noted that r_c is purely an operational figure of merit, which cannot be related to the barrier resistance or any other intrinsic property of the contact. However, it can be applied to any planar contact and is the quantity of interest to device and circuit designers.

We will now return to the specific contact resistivity ρ_c, as defined by Eq. (1.1.27). As will be discussed in more detail later, a metal–semiconductor junction can be described by a conduction-band diagram such as that shown for an n-type semiconductor in Fig. 1.1.21. Basically, an electron going from the metal to the semiconductor must go over an energy barrier $e\phi_B$, whereas an electron going the other way must traverse a barrier eV_{bi}, where V_{bi} is known as the *built-in* or *diffusion potential*; here, both ϕ_B and V_{bi} are defined as positive quantities. (For now we will ignore electrons going *through* the barrier). At equilibrium, Fig. 1.1.21(a), the electron currents j_{1e}

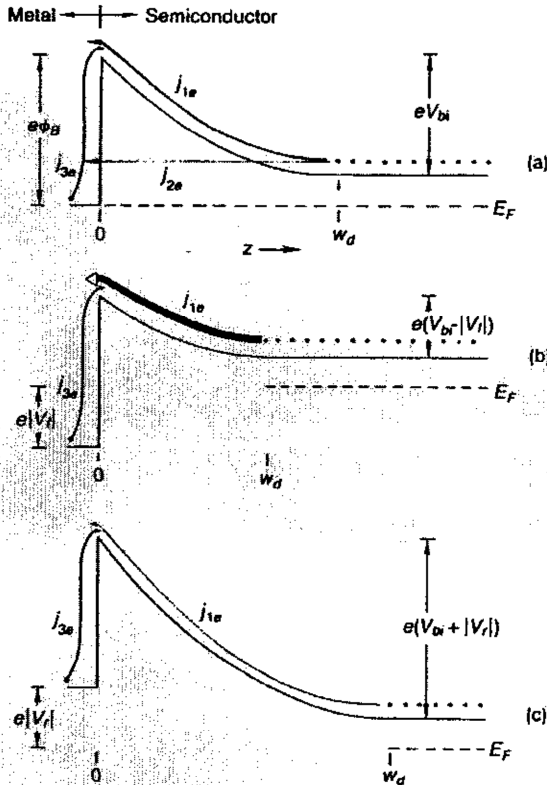

Fig. 1.1.21 The various electron-current components in a Schottky barrier under unbiased and biased conditions: j_{1e} and j_{3e} are injection currents and j_{2e} is a tunneling current. (a) No bias; (b) forward bias; (c) reverse bias

and j_{3e} will be of equal and opposite magnitudes because the net current must vanish. The currents j_{1e} and j_{3e} are known as thermionic currents, since it is the few electrons which have high thermal energies which can traverse the barriers. Let the Fermi energy in the neutral semiconductor region ($z \rightarrow \infty$) be defined as the zero of energy. Then when a positive voltage V_f is applied to the metal (a *forward* bias for an n-type semiconductor), its Fermi level will be lowered by $e|V_f|$ with respect to the semiconductor (Fig. 1.1.21b) and the $S \rightarrow M$ barrier will decrease to $e(V_{bi} - |V_f|)$, thereby raising j_{1e} by a factor $\exp(e|V_f|/kT)$. The $M \rightarrow S$ electron current j_{3e} remains the same, since its barrier does not change. Conversely, when a negative (*reverse*) bias is applied to the metal, the $S \rightarrow M$ barrier is raised by $e|V_r|$,

and the current j_{1e} is *decreased* by $\exp(e|V_r|/kT)$. Again, j_{3e} is unchanged to first order. The total situation can be described by the well-known diode equation

$$\begin{aligned} j(\text{ther.}) &= j_{rs}[\exp(eV/kT) - 1] \\ &= K_{rs} \exp(-e\phi_B/kT)[\exp(eV/kT) - 1] \end{aligned} \tag{1.1.28}$$

where j(ther.) is the conventional (positive) thermionic current density flowing from semiconductor to metal. Here j_{rs} is the *reverse-saturation current*, which is approximately constant for reverse bias (negative V) until breakdown begins to occur. It is clear that Eq. (1.1.28) does not represent an 'ohmic' contact except at very low voltages, for which

$$j = j_{rs}\frac{eV}{kT}, \qquad V \ll kT/e \tag{1.1.29}$$

However, the magnitude of j(ther.) is mainly limited by the $\exp(-e\phi_B/kT)$ term, since $e\phi_B \gg kT$ for GaAs at normal temperatures. Thus, if ϕ_B can be made small, then a high current density can be supported by a very small voltage drop across the contact, and that is what we really want in a contact.

The problem in GaAs is that ϕ_B cannot be made small by the proper choice of metal, evidently because of a high surface-state density. The alternative then is to make the barrier as *thin* as possible, in which case the tunneling current j_2, which was ignored before, can become appreciable. The $S \to M$ tunneling probability for electrons at the depletion edge is given by the familiar WKB approximation:

$$T(w_d) = \exp\left[-2\int_{w_d}^{0}\left\{\frac{2m}{\hbar^2}[\mathscr{E}(z) - \mathscr{E}(w_d)]\right\}^{1/2} dz\right] \tag{1.1.30}$$

where $\mathscr{E}(z)$ describes the shape of the barrier. As a fairly good approximation, the barrier is parabolic so that

$$\mathscr{E}(z) - \mathscr{E}(w_d) = e^2N(z - w_d)^2/2\epsilon$$

where N is the net donor concentration, ϵ is the dielectric constant, and w_d is the depletion depth, given by $w_d = [2\epsilon(V_{bi} - V)/eN]^{1/2}$. The integration therefore results in

$$T = \exp\frac{e(V - V_{bi})}{\dfrac{he}{4\pi}\left(\dfrac{N}{\epsilon m^*}\right)^{1/2}} \propto \exp\frac{e(V - V_{bi})}{\mathscr{E}_{00}} \tag{1.1.31}$$

where $\mathscr{E}_{00}$ is a standard designation in the literature. To compare the magnitudes of the tunneling and thermionic currents, note from Eq. (1.1.28) that

$$j(\text{ther.}) \propto j_{rs}\exp(eV/kT) \propto \exp[e(V - \phi_B)/kT]$$

for $eV \gg kT$, and note also that

$$j(\text{tun.}) \propto \exp\left[e(V - V_{bi})/\mathscr{E}_{00}\right].$$

Now V_{bi} and ϕ_B are not too different, and both $V - V_{bi}$ and $V - \phi_B$ are negative for all realistic values of V. Therefore, if $\mathscr{E}_{00} \gg kT$, then tunneling current will dominate, as illustrated in Fig. 1.1.22(b). For GaAs, $\mathscr{E}_{00} \simeq$

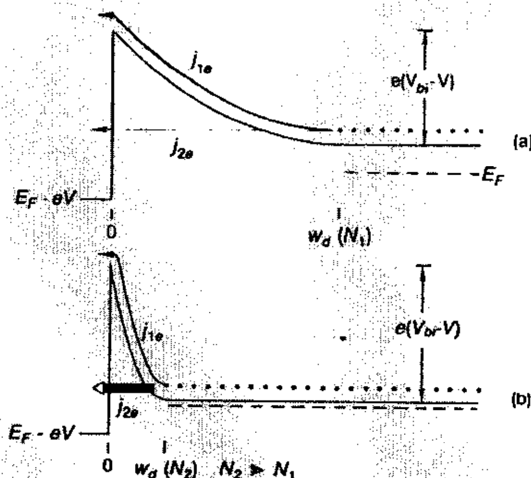

Fig. 1.1.22 The reduction of the depletion width w_d, and consequent increase of electron tunneling current j_{2e}, due to a much higher doping density, $N_2 \gg N_1$

$2.0 \times 10^{-11}\,N^{1/2}\,\text{eV}$, where N is in cm^{-3}. Therefore, $\mathscr{E}_{00} \gtrsim kT$ at $T = 300\,\text{K}$ when $N \gtrsim 1.6 \times 10^{18}\,\text{cm}^{-3}$. For even higher N we would expect that $\ln j(\text{tun.}) \propto \mathscr{E}_{00}^{-1} \propto N^{-1/2}$. This relationship is illustrated in Fig. 1.1.23 (Mead, 1969) for highly doped GaAs, showing that the theory has at least reasonable validity. Again, the tunneling phenomenon does not lead to an ohmic contact in the sense $j \propto V$, except for $eV \ll \mathscr{E}_{00}$. However, the important thing for most purposes is that a large current density be produced by a small voltage drop across the contact, and that will be true if N is large enough.

The tunneling current is commonly known as *field-emission current*, just as the 'over-the-barrier' current was known as *thermionic-emission current*. However, it is also possible to have a mixture, *thermionic-field-emission current*, which requires electrons to be thermally excited part way up the barrier, where they can then tunnel through the barrier, which is thinner at that point. These ideas are illustrated in Fig. 1.1.24 (Rideout, 1975), showing the regions of dominance of these three current modes as a function of T and N.

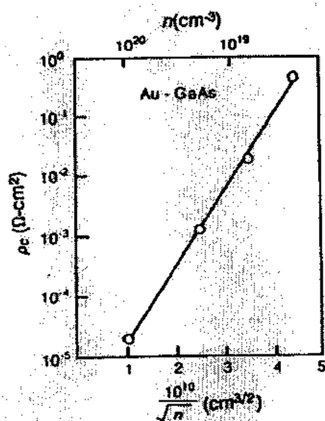

Fig. 1.1.23 Specific contact resistivity ρ_c of Au–Schottky barriers on n-type GaAs as a function of n for field-emission dominated conduction. (After Mead (1969). Reprinted by permission of the publisher, The Electrochemical Society, Inc)

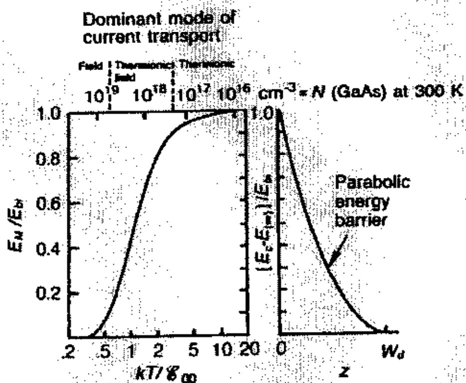

Fig. 1.1.24 Relative position of maximum transmission through or over a Schottky barrier vs the parameter $kT/\mathscr{E}_{00}$ (or n at 300 K). Note that field emission dominates for $n \gtrsim 5 \times 10^{18}\,\mathrm{cm}^{-3}$ at 300 K. (After Rideout, (1975). Reproduced by permission of Pergamon Press)

The recipe for an ohmic contact would then seemingly require either a small ϕ_B or a large N. Generally the latter option is more viable, and is usually implemented by using a thin n^+–GaAs region between the contact metal and the *active layer*. For example, a MESFET active layer would normally have $N = 2 \times 10^{17}\,cm^{-3}$, which by itself would not lead to a thin enough barrier. Thus, an n^+ layer with $N = 3 \times 10^{18}\,cm^{-3}$ is placed between the metal and the active layer. The working of such an ohmic contact is illustrated schematically in Fig. 1.1.25 for (b) forward bias (metal positive),

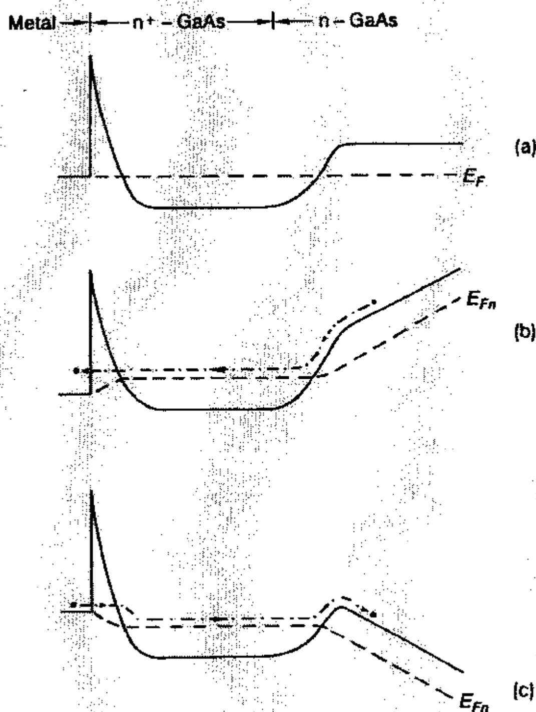

Fig. 1.1.25 Electron flow in a metal/n^+-semiconductor junction under forward bias (b), and reverse bias (c). In either case the current flows freely and thus the contact is ohmic

and (c) reverse bias (metal negative). In either case, the 0.8 eV barrier, $e\phi_B$, presents little resistance if N is large enough, and the n^+–n barrier (<0.3 eV) is not high enough to appreciably affect the reverse transport, except perhaps at very low temperatures.

Unfortunately, however, the tunneling model is not sufficient to explain the low values of contact resistivity being observed for present-day

metal/semiconductor junctions in GaAs, probably because most of these junctions are alloyed, and thus not strictly planar. The most popular metallization is composed of Au, Ge, and Ni, and will be described in more detail later. However, Fig. 1.1.26 (Braslau, 1981) shows that typical values

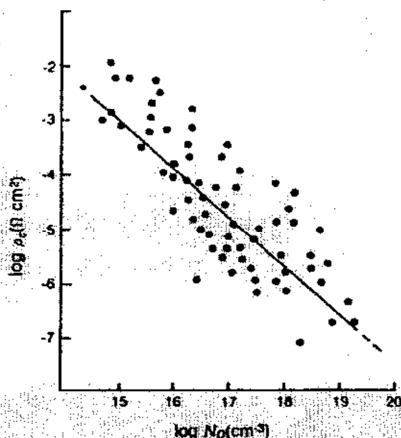

Fig. 1.1.26 The relationship of ρ_c to N_D for contact results from many different laboratories. The results appear to follow Eq. (1.1.32). (After Braslau (1981). Reproduced by permission of The American Institute of Physics)

of ρ_c for this material are much lower for a given N than would have been predicted by the tunneling model (see Fig. 1.1.23). Also, it appears that $\rho_c \sim N^{-1}$, rather than $\log \rho_c \sim N^{-1/2}$. It is perhaps not surprising that the tunneling model fails here when the interface in such a contact is examined. For example, in Fig. 1.1.27 (Shih *et al.*, 1987) it is seen that the metal

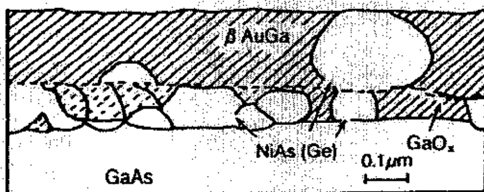

Fig. 1.1.27 The various material phases present after annealing an AuGeNi contact at 440°C for 2 min. (After Shih *et al.*, (1987). Reproduced by permission of The American Institute of Physics)

elements have mixed with the Ga and As in a very complicated way, and have formed several new compounds in the process. In fact, it sometimes appears that spikes of highly doped material are protruding into the GaAs, and that the current mainly transfers through these spikes. Braslau (1981) has formulated a model to take account of these spikes, as illustrated in Fig. 1.1.28. Here it is assumed that the metal makes contact with the protrusions, which are modeled as hemispheres of average radius $\langle r \rangle$, and have an average density $1/\langle A \rangle^2$. Then the barrier resistance per hemisphere is given by $R_c = \rho_c/2\pi\langle r \rangle^2 f$, where f is a field-enhancement factor ($f \gtrsim 1$) to take account of the non-uniform field distribution of the protrusion. To the barrier resistance we must add a spreading resistance per hemisphere of $\rho/\pi\langle r \rangle$, where ρ is the resistivity of the GaAs underneath. The total

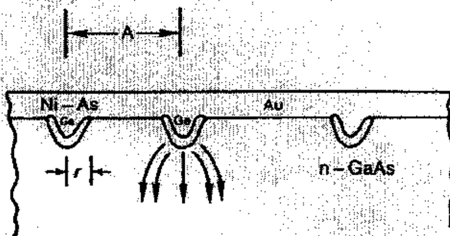

Fig. 1.1.28 A model for ohmic contacts in which conduction takes place through a parallel array of Ge-rich protrusions. (After Braslau (1981). Reproduced by permission of The American Institute of Physics)

effective specific contact resistivity is then

$$\rho_c^{\text{eff}} = \langle A \rangle^2 \left\{ \frac{\rho}{\pi\langle r \rangle} + \frac{r_c}{2\pi\langle r \rangle f} \right\} \tag{1.1.32}$$

The second term is considered negligible if $\rho > 10^{-3}$ Ω-cm, so that $\rho_c^{\text{eff}} \propto \rho \propto (\mu N)^{-1}$ in that case. Thus, this model can explain the dependence of ρ_c on N, and also predicts that ρ_c can be decreased by decreasing $\langle A \rangle$, i.e., by producing more protrusions per unit area. However, that is a difficult task since it is not even known what produces the protrusions, and furthermore, there are cases (cf. Fig. 1.1.27) where they do not seem to be necessary to form a good ohmic contact. Further work will be necessary to understand this problem completely.

A final method of making ohmic contacts in GaAs should be discussed. Although we previously discounted the possibility of making $e\phi_B$ much less than 0.8 eV (see, however, Section 1.1.7.3.1 and Iliadis (1987)), there is a way of getting a lower 'effective' ϕ_B which is becoming increasingly popular.

This novel method makes use of a different semiconductor material, such as InAs, which either has an electron affinity $e\chi$ *greater* than the metal work function $e\phi_m$, or has surface states which pin the Fermi level *near* the conduction band. The barrier $e\phi_B$ is then small, as illustrated in Fig. 1.1.29(b) (Woodall *et al.*, 1981), unlike the GaAs case (Fig. 1.1.29a) for

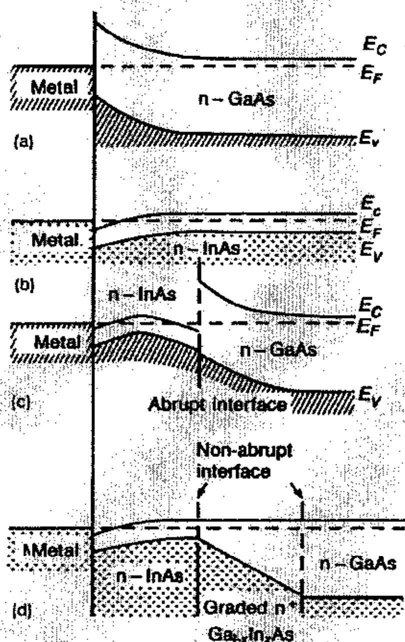

Fig. 1.1.29 Band diagrams for various semiconductor interfaces: (a) metal on n-GaAs; (b) metal on n-InAs; (c) metal on n-InAs on n-GaAs; (d) metal on n^+-InAs on graded n^+-$Ga_{1-x}In_xAs$ on n-GaAs. (After Woodall *et al.* (1981). Reproduced by permission of The American Institute of Physics)

which $e\phi_B$ is large. Thus, electrons can move easily between the metal and InAs. When the InAs is put between the metal and GaAs (Fig. 1.1.29c) then a conduction-band discontinuity exists and impedes the electron flow. If, however, the InAs is graded from InAs$\rightarrow In_xGa_{1-x}As\rightarrow$GaAs, then the electrons can once again flow freely. This model may offer an explanation of why pure In has always proved to be a good contact for n-type GaAs (Lakhani, 1984; Allen *et al.*, 1987), even though it is isoelectronic with Ga, and thus not a donor. If the In metal alloys with the GaAs, and forms a

graded heterojunction, then it might make an ohmic contact in the way depicted in Fig. 1.1.29. However, the major interest in the heterojunction method at present is to make *non-alloyed* contacts, in which case the InAs or $In_xGa_{1-x}As$ is epitaxially grown onto the GaAs, and then the metal is evaporated on, without heating. The major advantage here is for small-dimension devices in which neither vertical nor lateral diffusion due to the alloying process can be tolerated.

1.1.7.3 Practical ohmic contacts for GaAs

So far we have discussed the definition and theory of ohmic contacts. However, it is probably even more important for the purposes of this book to give some practical methods for making such contacts. As stated earlier, the total current necessary for a given signal strength in a Hall-effect measurement is approximately constant as the Hall-pattern dimensions are scaled down. Thus, the current *density* that the contacts must handle is much higher for the small pattern, and better ohmic contacts are necessary. It is reasonable, therefore, to discuss the large-area and small-area cases separately.

1.1.7.3.1 Contacts for small devices. Contact fabrication procedures for small devices are continually changing as the device dimensions decrease. However, the 'work-horse' metallization for GaAs, and for other III–V compounds such as $Al_xGa_{1-x}As$, is the AuGe eutectic (88% Au, 12% Ge) which melts at about 360°C. Up until recent times, it has been believed that this metal produces an ohmic contact by means of Ge diffusion into the GaAs, and subsequent Ge_{Ga} donor formation, which then makes the required n^+ layer, as discussed in the last section. It has also been believed that placing a Ni overlay on the AuGe is helpful because it inhibits the 'balling-up' of the AuGe. However, it is now realized that the situation is much more complex than this. For example, there is evidence (Iliadis, 1987), to suggest that the Ge indeed produces n^+ doping, but also that it induces disorder, even below the Au–Ge eutectic temperature, and through this process reduces ϕ_B. Thus, both enhanced tunneling and barrier-lowering are serving to reduce the contact resistance. At higher temperatures, several new compounds, such as NiAs:Ge, are formed and play important roles. Furthermore, 'protrusions' of the NiAs or other compounds may be necessary for the best results. Thus, it is clear that this system is still not completely understood; however, it is the one most commonly used today, and perhaps for the foreseeable future. One fairly convenient 'recipe' for such contacts, due to Braslau, is reproduced in Shur (1987), p. 151. A somewhat more complicated recipe, involving sputter cleaning (Callegari *et al.*, 1985), produces more stable and reliable contacts; the details are given in Table 1.1.3. Other recipes may be found in the literature cited in Table 1.1.4.

Table 1.1.3 Fabrication of reliable AuGeNi ohmic contacts to n-type GaAs by sputter cleaning before deposition. (After Callegari *et al.* 1985. Reproduced by permission of the American Institute of Physics.)

(1) Evacuate evaporation system to 2×10^{-5} Pa; then fill with O_2 to 5.3 Pa
(2) Sputter clean with O_2 gas for about 5 min at about 100 V d.c.
(3) Pump out O_2 and fill with Ar at 1.3 Pa.
(4) Sputter clean with Ar for about 5 min at about 250 V d.c.; then pump system below 10^{-5} Pa.
(5) Deposit, sequentially, 5 nm of Ni, 100 nm of eutectic AuGe, 30 nm of Ni, and 50 or 100 nm of Au.
(6) Alloy in furnace for about 3 min at about 420°C, in an $Ar/H_2(H_2 10\%)$ gas mixture.

A problem with the AuGe:Ni system is that high-temperature (>400°C) alloying is usually necessary, thus producing an inhomogeneous interface, and some lateral spreading, which can be detrimental in many cases. Thus, some lower-temperature furnace and surface-heater processes have been investigated (Kuzuhara *et al.*, 1985), as well as laser annealing (Imanaga *et al.*, 1987), and some other processes that require no annealing at all (Kalkur *et al.*, 1985). Furthermore, many other metal systems besides AuGe:Ni have been studied. It is beyond the scope of this book to discuss these new processes and metals in great detail, but we do list a large number of the recent (mostly 1986 and 1987) literature results in Table 1.1.4. Earlier reviews (Rideout, 1975; Piotrowska *et al.*, 1983) cover much of the previous time period. Results for p-type GaAs and a few ternary III–V compounds involving Ga and/or As are also included in Table 1.1.4. It should be noted that most workers have used the same contacting procedures for the important ternary $Al_xGa_{1-x}As$ as for GaAs. Also, as discussed earlier, much progress has been made with In compounds, probably due to the formation of a graded $In_xGa_{1-x}As$ layer, which avoids the formation of high barriers in the interface region. For example, Allen *et al.* (1987) have achieved specific contact resistivities of less than 1×10^{-6} Ω-cm^2 with In/Pd metallization by using rapid thermal annealing (RTA) at 500°C for 20 s. A further advantage of In contacts is their high-temperature (up to 900°C) stability (Otsuki *et al.*, 1988).

1.1.7.3.2 Contacts for larger structures. For typical bulk Hall-effect patterns, with mm or even cm dimensions, the contacts can be made large enough that the current densities are not high. For such cases it is not necessary to have specific contact resistivities of 10^{-6} Ω-cm^2, although some workers still prefer the use of AuGe, which requires evaporation. An old method, which we have found very useful, and still use routinely in our laboratory, is to solder pure In onto the sample, say at the corners of a van der Pauw square, and then anneal at about 425°C for 2–3 min in a flowing inert gas (Ar or N_2). For semi-insulating GaAs, it is not necessary to anneal

the contact at all. It has been our experience that soldered In will wet any clean, polished GaAs surface, without use of an ultrasonic iron. Some workers prefer In/Sn, of mixtures from 5 to 50% Sn, for n-type GaAs, and In/Au or In/Zn, with about 5% Au or Zn for p-type GaAs; such alloys are also easily soldered. A reasonable procedure for this type of contact is outlined below:

(1) Clean sample surface, if necessary, with a trichloroethylene, acetone, methanol, and DI water sequence, or other standard procedure.
(2) Apply In or In/Sn, for n-type samples, and In or In/Au, for p-type samples, with a small soldering iron. Generally the surfaces are wetted immediately.
(3) Anneal at 425°C for 2 min in flowing Ar or N_2. This step is usually not necessary for semi-insulating GaAs.

In our laboratory, we have found that if this technique does not produce a low-resistance contact on a particular sample, then neither will evaporated AuGe or any other metal. That is, if In fails as a contact, then the material itself is probably inhomogeneous and non-ohmic.

For semi-insulating GaAs, it is sometimes possible to get by with very crude contacts, since the current densities will normally be very low. For example, unalloyed In, silver paste, and even a conductive rubber (Kuhnel *et al.*, 1987) have been used. However, the ohmic nature of the contacts should always be tested by reversing the current and magnetic-field polarities, and by varying the current magnitude.

1.1.8 Apparatus

1.1.8.1 General considerations

Hall-effect measurements in conductive GaAs may be performed with very simple and inexpensive apparatus. For example, reasonably good values may be obtained for 1 Ω-cm, bulk, n-type material with a battery, 500 G bar magnet, and a common multimeter, which can all be purchased for less than $100. In contrast, a large, fully automated apparatus, which can handle semi-insulating samples (say, 10^{10} Ω), and which is interfaced with a closed-cycle He cryogenic system, can cost as much as $100 000. The basic instruments needed for all Hall-effect experiments are a current (or voltage) source, ammeter, voltmeter, magnet, and also a switchbox if van der Pauw measurements are to be performed. Beyond that, however, several factors need to be considered:

1.1.8.1.1 sample size
1.1.8.1.2 measurement temperature and pressure
1.1.8.1.3 impedance levels
1.1.8.1.4 magnetic-field strength
1.1.8.1.5 requirements for photo-excited measurements
1.1.8.1.6 automation.